International Journal of Mechanical and Production Engineering Research and Development (IJMPERD)
ISSN (P): 2249–6890; ISSN (E): 2249–8001
Vol. 11, Issue 4, Aug 2021, 27-46

MODELING, SIMULATION AND OPTIMIZATION OF A REVERSE OSMOSIS DESALINATION PLANT

RANDY NCUBE & FREDDIE L. INAMBAO

Department of Mechanical Engineering, University of Kwazulu-Natal, Durban, South Africa

ABSTRACT

Reverse osmosis modeling and simulation is essential in the design of a seawater reverse osmosis desalination plant. Proper procedures will result in designs that will help engineers and designers to come up with optimized plants. This article gives modeling, simulation and optimization of the V & A desalination plant located in Cape Town, South Africa. Mathematical modeling was assumed to be following the basic principles and equations of mass and transport theory. Simulation and optimization were accomplished using Water Application Value Engine simulation software. The optimization results showed a 7.3 % improvement in specific energy consumption (SEC) and about 18 % improvement in permeate productivity using the same membranes, recovery rate and feed total dissolved solids.

KEYWORDS: Desalination, Reverse Osmosis, Modeling, Simulation, Optimization & WAVE Software

Received: Mar 13, 2021; **Accepted**: Apr 23, 2021; **Published**: Jun 11, 2021; **Paper Id.**: IJMPERDAUG20213

Original Article

1. INTRODUCTION

Potable water scarcity is proving to be a global problem as the number of people with inadequate supply of fresh water keeps on increasing. South Africa is also faced with this problem. The drought in 2018 was the worst recorded in the country, and the city of Cape Town is now exploring alternative sources of potable water supply and water management systems (Enqvist & Ziervogel, 2019). One of the alternatives is desalination of brackish and seawater, particularly by means of seawater reverse osmosis (SWRO) desalination. RO has taken leadership in the desalination market (Lappalainen et al., 2017). At least 60 % of the world's total installed desalination plants are RO operated (Ahmed et al., 2019). RO plant performance is sensitive to input parameters such as feed water quality and operating conditions (Oh et al., 2009). Energy consumption is one of the most important parameters that is still relatively high in the RO desalination process and this needs to be minimized. Optimization of the plants that are in operation is one of the ways that will help in minimizing the SEC, at the same time optimizing the desalination system. This paper seeks to develop a software-based model for simulation and optimization with respect to the already operational plant.

2. MODELING OF THE PLANT

Modeling is a procedure in which mathematical equations are used to describe real-life problems so as to solve these problems more easily (Ahmed et al., 2019). RO modeling, if done properly, will result in fewer experiments needing to be undertaken, thereby reducing time and costs associated with desalination (Ang & Mohammad, 2015). Several modeling techniques are applied to come up with mathematical relationships between the different parameters. Membrane modeling software is often used to estimate the performance of the system but is limited to membranes that are designed by a specific company. Coupling of different software or membrane manufacturers is

not possible yet (Altaee, 2012). Modeling of the RO plant in this study follows the following assumptions:

- The pressure drop is neglected along the membrane channel.
- Spiral wound elements are treated as flat.
- The concentration of feed linearly varies along the feed channel (Sassi & Mujtaba, 2010).

This section assumes that the plant follows the modeling equations that are listed in the equations below. In the solution diffusion model, permeate flow rate, Q_w, is calculated using Eq. 1:

$$Q_w = A(\Delta P - \Delta\pi) \quad \text{(Eq. 1)}$$

Where ΔP is feed and permeate pressure difference and Δπ is osmotic pressure (Ahmed et al., 2019; Kim, Oh et al., 2009; Oh et al., 2009).

Osmotic pressure, Δπ equation is given by Eq. 2:

$$\Delta\pi = n_i C R_g T \quad \text{(Eq. 2)}$$

Where n_i, R_g and T represent number of moles of species, universal gas constant 0.082 kg.m^2/h^2.K and feed temperature respectively.

The recovery ratio, K, is given by Eq. 3:

$$K = \frac{Q_p}{Q_f} \quad \text{(Eq. 3)}$$

Where Q_p is permeate flow and Q_f is feed flow. The recovery ratio tends to decrease with an increase in feed total dissolved solids (TDS) at a given temperature (Nisan et al., 2005).

The temperature correlation factor (TCF) for a given RO plant is calculated by Eq. 4:

$$TCF = e^{\left[\frac{E_m}{R}\left(\frac{1}{273+T}-\frac{1}{298}\right)\right]} \quad \text{(Eq. 4)}$$

Where E_m is membrane activation energy, R is gas constant and T is temperature (Atab et al., 2016).

The theoretical calculations of SEC and permeate flux (J_v) are given by Eq. 5 and Eq. 6 respectively (Assad et al., 2020):

$$SEC = \frac{E_{bp} + E_{hp} + E_{sp}}{Q_p} \quad \text{(Eq. 5)}$$

$$J_v = \frac{Q_p}{A} \quad \text{(Eq. 6)}$$

Where: E_{bp}, E_{hp} and E_{sp} are energies consumed by the booster pump, high pressure pump and supply pump respectively, and Q_p and A represent the permeate water flow rate and area of membrane respectively.

Salt rejection, R_s, and total mass balance, Q_fC_f are calculated respectively by Eq. 7 and Eq. 8. Permeate water flow rate is calculated by Eq. 9 and Eq. 10:

$$R_s = 1 - \frac{TDS_p}{TDS_f} \quad \text{(Eq. 7)}$$

$$Q_f C_f = Q_p C_p - Q_r C_r \quad \text{(Eq. 8)}$$

$$Q_p = Q_f - Q_r \quad \text{(Eq. 9)}$$

$$Q_p = n_i W \int_0^L J_v dz \quad \text{(Eq. 10)}$$

Where C_f, C_p and C_r are feed, permeate and reject salts mass concentrations respectively, Q_r is reject water flow rate and n_i, L and W represent number of leaves, length and width of the RO module.

Accordingly, solvent flux, J_v, and solute flux, J_s follow the following expressions:

$$J_v = A_w\left(P_f - P_d - P_p - \Delta\pi\right) \quad \text{(Eq. 11)}$$

$$J_s = B_S(C_m - C_b) \quad \text{(Eq. 12)}$$

Where A_w represents the solvent transport parameter, P_f, P_d and P_p represent feed pressure, pressure drop along the membrane and permeate pressure (Ang & Mohammad, 2015; Jiang et al., 2014; Swartz et al., 2006).

Impermeable salt accumulation on membrane surfaces leads to concentration polarization, ϕ, given by Eq. 13:

$$\emptyset = \frac{C_m - C_p}{C_b - C_p} = e^{\frac{J_v}{k}} \quad \text{(Eq. 13)}$$

Where C_b is bulk solution solute concentration and k is the mass transfer concentration (Lee et al., 2010).

Normalized Temperature, TMP*:

$$TMP^* = TCF * TMP \quad \text{(Eq. 14)}$$

Temperature correction factor (TCF) is a factor that takes into cognisance the effect of the temperature (Gilabert Oriol et al., 2013).

Specific energy consumption (SEC) of the plant is calculated using Eq. 15 and Eq. 16 respectively:

$$SEC = \frac{W_{pump}}{Q_p} \quad \text{(Eq. 15)}$$

$$W_{pump} = \frac{\Delta P * Q_f}{\eta_{pump}} \quad \text{(Eq. 16)}$$

Where W_{pump} is the work done by the pump and η_{pump} is the pump efficiency (Zarai et al., 2013).

3. SIMULATION

In the following section, the above modeling equations are applied to the simulations performed. Simulation was conducted on the data using DuPont powered Water Application Value Engine (WAVE) software, modeling software for water treatment plant design. WAVE is a fully integrated modeling software that integrates three main leading water treatment technologies. These include reverse osmosis (RO), ultrafiltration (UF) and ion exchange (IU) (DuPont, 2021). The software combines the previous software features of reverse osmosis system analysis (ROSA), offering improved and consistent algorithms, improved mass balance and flow resulting from temperature changes, water characteristics and water compressibility and sharing of designs is also possible (Edina, 2017).

Simulations for the 100-10 train were carried out. Most of the variables were extracted from experimental values and some of the values were assumed before performing the simulations. One of the parameters assumed was the permeate water flow, $Q_{permeate}$. The assumption was that all three trains produce equal amounts of permeate water, therefore the total permeate flow rate of 1 367 m^3/d was divided into three equal parts, resulting in each train producing approximately 460 m^3/d or 20 m^3/h. DOW SW30 ULE 440i membranes are now obsolete therefore all the membranes were assumed to be DOW SW30 XLE 440i. Table 1 shows experimental values and assumptions made on the plant.

Table 1: Assumed and Experimentally Extracted Values for Different Parameters

Parameter	Assumed Value	Experimental Value
Q_{feed} [m^3/d (m^3/h)]	460 (20)	
$Q_{permeate}$ [m^3/d (m^3/h)]	1480 (62)	
Average temperature, (T/ °C)	14.5	
Average pH	7.2	
Average pressure (P/ bars)	55	
Recovery (%)		31
Feed TDS (mg/l)		33728
DOW SW30 XLE 440i	7 membranes	
DOW SW30 ULE 440i		(Obsolete)
No. of vessels		6

Table 2: Simulated Results of the V & A Desalination Plant

Parameter	V & A Desalination Plant	Simulated Value	Error (%)
Permeate flow (m^3/h)	19	20	5
Feed TDS (mg/l)	33 728.88	33 619	0.3
Permeate TDS (mg/l)	399.79	104	73
Feed pressure (bars)	55	46.7	15
Energy consumption (kW/h)	6.58	5.68	13.7
Peak power (kW)	125	113.5	9.2
Recovery (%)	31	31	0
Rejection (%)	98.81	99.69	0.9

The schematic diagram and the description of variables of the simulated results are shown in Figure 1. and Table 3 respectively. Stage 1 shows the raw feed water inlet and stage 2 shows the pressurized feed water to the RO vessels. Stages 3, 4 and 5 indicate concentrate water. Some of the concentrate is recycled back to feed water (stage 3) whilst some of the concentrate is discarded as waste (Stage 5). Stage 6 shows the permeate (potable water). At every stage of the simulation, TDS and pressures are recorded. Feed pressure is recorded as 46.4 bar (stage 2) compared to the experimental value of 55 bar.

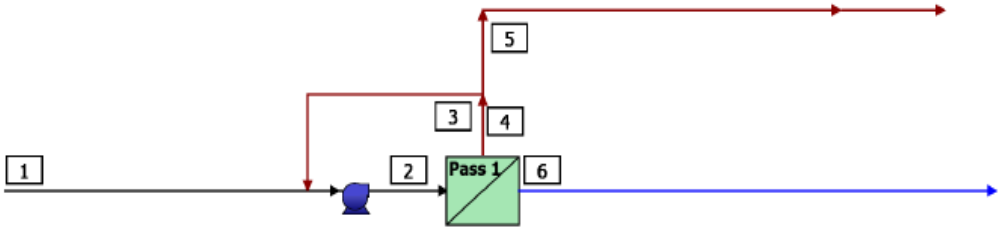

Figure 1: Schematic Diagram of the Simulated Design.

Table 3: Description of Different Stages of Simulation and their Corresponding Values

#	Description	Flow (m^3/h)	TDS (mg/L)	Pressure (bar)
1	Raw Feed to RO System	64.5	33,619	0.0
2	Net Feed to Pass 1	69.3	34,750	46.4
3	Concentrate Recycle from Pass 1 to Pass 1	4.94	48,751	43.6
4	Total Concentrate from Pass 1	49.4	48,751	43.6
5	Net Concentrate from RO System	44.4	48,751	43.6
6	Net Product from RO System	20.0	117.8	0.0

A summary of the simulation results system overview and flow table is shown in Tables 4 and 5 respectively. These results show several deviations to the values extracted from the actual plant. Ideal SEC was recorded as 5.6 kWh/m^3, while the actual SEC of the plant is 6.58 kW/h, a higher value. An average flux of 11.6 LMH and permeate TDS of 117.8 mg/l was recorded.

Table 4: RO System Overview

Pass		Pass 1
Stream Name		Stream 1
Water Type		Sea Water (With conventional pretreatment, SDI < 5)
Number of Elements		42
Total Active Area	(m^2)	1717
Feed Flow per Pass	(m^3/h)	69.3
Feed TDS[a]	(mg/L)	34,750
Feed Pressure	(bar)	46.4
Flow Factor Per Stage		0.85
Permeate Flow per Pass	(m^3/h)	20.0
Pass Average flux	(LMH)	11.6
Permeate TDS[a]	(mg/L)	117.8
Pass Recovery		28.9 %
Average NDP	(bar)	13.3
Specific Energy	(kWh/m^3)	5.60
Temperature	(°C)	16.0
pH		7.2
Chemical Dose		-
RO System Recovery		31.0 %
Net RO System Recovery		31.0%

Table 5: RO Flow Table

Stage	Elements	#PV	#Els per PV	Feed				Concentrate			Permeate			
				Feed Flow (m^3/h)	Recirc Flow (m^3/h)	Feed Press (bar)	Boost Press (bar)	Conc Flow (m^3/h)	Conc Press (bar)	Press Drop (bar)	Perm Flow (m^3/h)	Avg Flux (LMH)	Perm Press (bar)	Perm TDS (mg/L)
1	SW30XLE-440i	6	7	69.3	4.94	46.0	0.0	49.4	43.6	2.5	20.0	11.6	3.0	117.8

A detailed report on the simulation is provided in Appendix A. This includes the behavior of each RO element (membrane) during the operation, several solute concentrations, electricity costs, utility and specific water costs.

The following section is dedicated to graphs that were obtained from the WAVE simulation project (Figure. 2 to Figure 6).

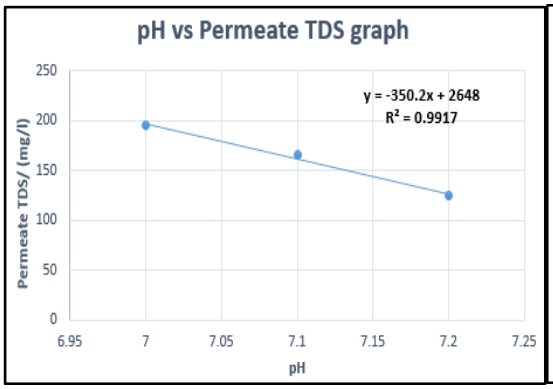

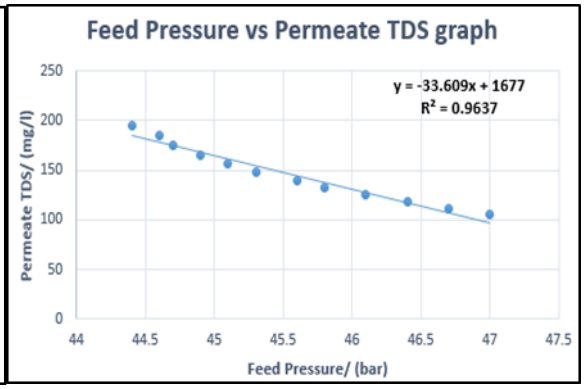

Figure 2: pH vs Permeate TDS Graph **Figure 3: Permeate TDS as a Function of Feed Pressure.**

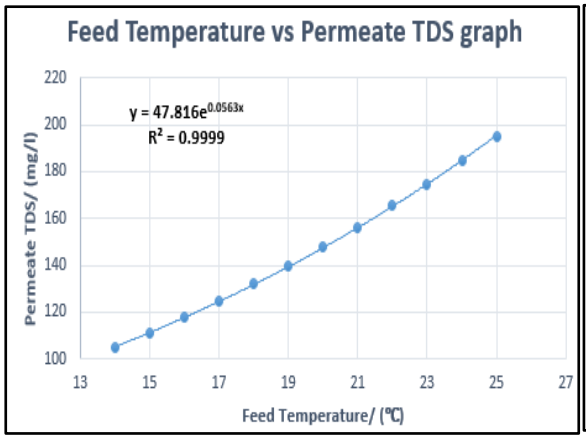

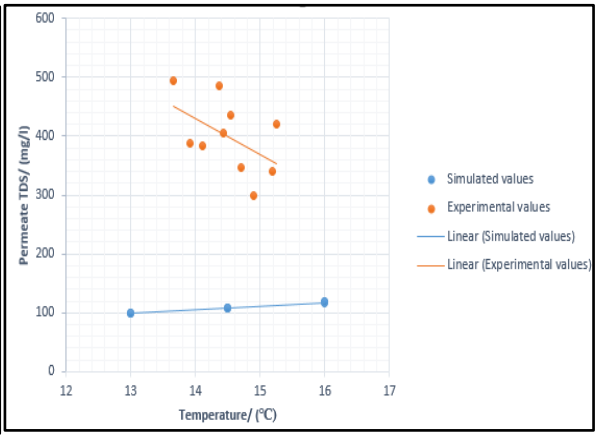

Figure 4: Feed Temperature and Permeate TDS Relationship **Figure 5: Simulated vs Experimental Values of Feed Temperature vs Permeate TDS.**

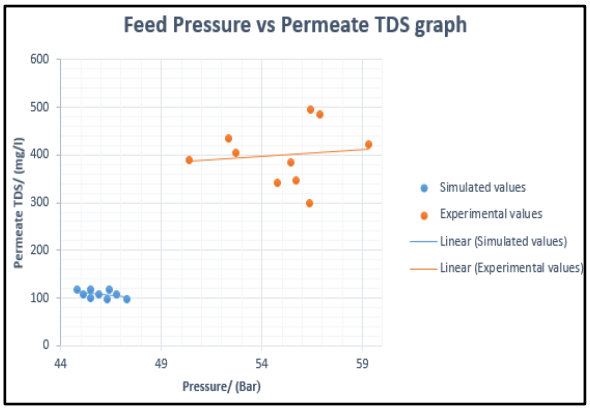

Figure 6: Simulated vs Experimental Values of Feed Pressure vs *Permeate TDS.*

4. OPTIMIZATION

Optimization is a procedure undertaken to come up with the best possible solution to a problem by using different alternatives (Ahmed et al., 2019). Some of the optimization techniques include the genetic algorithm (GA) technique

(Poullikkas, 2001; Murthy & Vengal, 2006; Djebedjian et al., 2008), artificial neural network (ANN) based modeling (established by Libotean et al., 2009). Optimization of the energy consumption is one of the key parameters as energy consumption accounts for 50 % to 60 % of total costs (Ahmed et al., 2019). Parameters like feed pressure and operational temperature as well as membrane properties affect the performance of RO process (Jiang et al., 2014).

Djebedjian et al. (2008) state that for optimization, the single objective to be maximized, Z, and the constraint used in the RO system, C_p, are given by Eq. 17 and Eq. 18 respectively:

$$Z = Q_w \qquad (Eq.17)$$

$$C_p \leq C_{p,d_i} \qquad (Eq.18)$$

If external penalty is used in the conversion of constrained problem to an unconstrained problem, then Z is given by Eq. 19:

$$Z = Q_w - Pen \qquad (Eq.19)$$

Where Pen is the penalty subtracted from the objective function and is given by Eq. 20:

$$Pen = C_{pen}\left(\frac{C_p}{C_{p,d}} - 1\right) \qquad (Eq.20)$$

Where C_{pen} represents the penalty function constant (can be as big as 100 000).

From the above equations, objective fuction, Z, is expressed by Eq. 21:

$$Z = \begin{cases} Q_w \; if \; C_p \leq C_{p,d} \\ Q_w - C_{pen} * \left(\frac{C_p}{C_{p,d}} - 1\right) \; otherwise \end{cases} \qquad (Eq.21)$$

Sassi and Mujtaba (2011) stated that optimization strategy considering module design and operating parameters is given by the following method:

Given: Membrane properties and specifications and feed water characteristics (conditions),

Optimize: The optimal feed flow, feed pressure and design decisions,

So as to minimize: Specific energy consumption,

And maximize: Permeate flow,

Subject to: Equality and inequality constraints.

Optimization was conducted using the WAVE modeling and optimization software. Optimization of the V & A desalination plant was performed so as to come up with the best combination of variables. The plant was operating at around 68 % of the design capacity, (1 367 m^3/d instead of the design capacity of 2 000 m^3/d). Optimization of the 100-10 train resulted in an increase of the operating capacity to around 86 % capacity, using the same equipment with the same recovery rate of 31 %. Specific energy was improved from 6.58 kWh/m^3 to around 6.1 kWh/m^3, an improvement of around 7.3 %.

The schematic diagram in Figure 1 applies to the optimization of the plant. Feed flow rate was increased to 83.2 m^3/h resulting in a permeate flow rate of 24 m^3/h at a pressure of 50.5 bars compared to the current permeate flow of

around 19 m^3/h at 55 bars. Although most of the parameters showed positive changes, specific water costs increased slightly, by 2 %. The summary of input and output parameters is shown in Table 6 and Table 7. Table 6 shows the RO optimization system overview, a set of input parameters, and expected output values. Table 7 depicts the RO optimization flow figures. Appendix B shows a detailed optimization report of the 100-10 plant.

Table 6: RO Optimization System Overview

Pass		Pass 1
Stream Name		Stream 1
Water Type		Sea Water (With conventional pretreatment, SDI < 5)
Number of Elements		42
Total Active Area	(m^2)	1717
Feed Flow per Pass	(m^3/h)	83.2
Feed TDS[a]	(mg/L)	34,752
Feed Pressure	(bar)	50.5
Flow Factor Per Stage		0.85
Permeate Flow per Pass	(m^3/h)	24.0
Pass Average flux	(LMH)	14.0
Permeate TDS[a]	(mg/L)	82.80
Pass Recovery		28.8 %
Average NDP	(bar)	17.3
Specific Energy	(kWh/m^3)	6.10
Temperature	(°C)	13.0
pH		7.3
Chemical Dose		-
RO System Recovery		31.0 %
Net RO System Recovery		31.0%

Table 7: RO Optimization Flow Table

Stage	Elements	#PV	#Els per PV	Feed				Concentrate			Permeate			
				Feed Flow (m^3/h)	Recirc Flow (m^3/h)	Feed Press (bar)	Boost Press (bar)	Conc Flow (m^3/h)	Conc Press (bar)	Press Drop (bar)	Perm Flow (m^3/h)	Avg Flux (LMH)	Perm Press (bar)	Perm TDS (mg/L)
1	SW30XLE-440i	6	7	83.2	5.92	50.2	0.0	59.2	46.9	3.4	24.0	14.0	3.0	82.80

The following graphs are the optimization graphs of permeate TDS against feed temperature, feed pressure and feed pH. The graph of permeate TDS and feed temperature (Figure 7) shows a general increase in permeate TDS as temperature increases, while the graph of feed pressure and permeate TDS (Figure. 8) shows a decrease in salt content with respect to an increase in pressure. An increase in pH resulted in a decrease in permeate TDS as shown in Figure. 9.

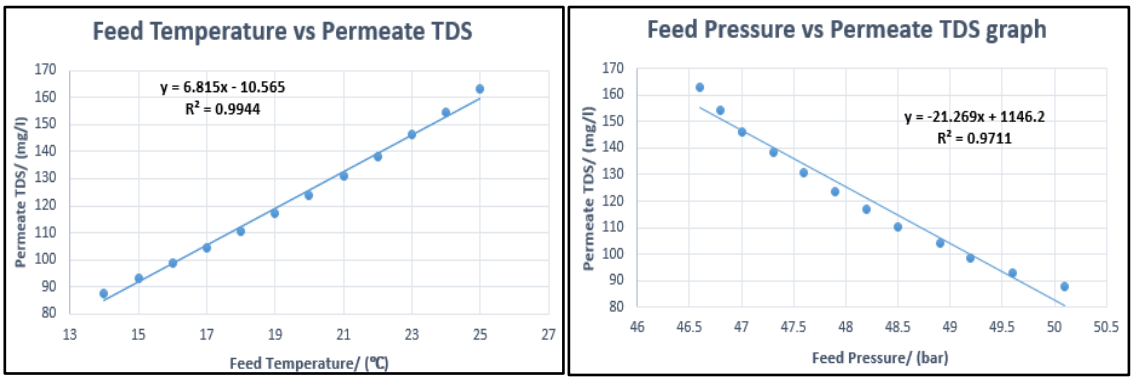

Figure 7: Permeate TDS as a Function of Feed Temperature. Figure 8: Feed Pressure and Permeate TDS Relationship.

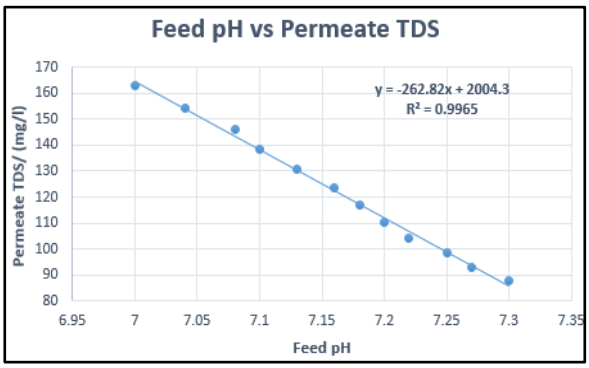

Figure 9: Feed pH Against Permeate TDS Graph.

5. DISCUSSIONS

The main objective of optimization is the minimization of energy consumption of the plant, without compromising the quality of the permeate water. To achieve the theoretical SEC is not possible due to concentration polarization, hydraulic resistance and membrane fouling (Gude, 2011). Optimization of the V & A desalination plant using WAVE software resulted in a decrease of about 13.7 % compared to the experimental value. This decrease in SEC will lead to a reduction in total costs of the plant. The optimization graph on Figure. 7 shows that an increase in temperature resulted in an increase in permeate TDS. This means that a decrease in temperature will result in improved permeate water quality. This is in agreement with Guler et al. (2010) who stated that a decrease in temperature enhances the quality of permeate water. According to Koutsou et al. (2020) increasing temperature of high saline water negatively impacts the salt rejection capabilities of the membranes, hence optimization studies have to be considered. Membrane performance generally decreases with an increase in temperature, thereby increasing the permeate TDS with respect to temperature increase (Kim, Lee et al., 2009; Kim et al., 2020; Kim et al., 1919). This increase in permeate TDS is due to an increase in the viscosity of the water (Kim, Lee et al., 2009) and the expansion of the membrane pores (Atab et al., 2018). Khalifa et al. (2017) are in agreement with the theory that an increase in temperature increases permeate flux resulting in high permeability of membranes and an increase in permeate TDS.

In recent years, high permeate water quality has been expected to be produced from SWRO desalination plants. Permeate water with TDS as low as 200 mg/l or less after re-mineralization is the expected quality (Kim et al., 2020). Optimization of the V & A plant resulted in a permeate TDS of around 82 mg/l (Table 6 and Table 7), which is very desirable. On the other hand, an increase in temperature results in a reduction in SEC and an increase in recovery ratio (Atab et al., 2018).

Figure 8 shows that feed pressure is directly proportional to the quality of product water. This means that as feed pressure increases, permeate TDS generally decreases, leading to improved quality of water produced. This is in agreement with Lee et al., (2015) and Du et al. (2020) who stated that an increase in feed pressure increases permeate flux and salt rejection while at the same time reducing SEC. Gandhidasan and Al-Mojel (2009) also agree that an exponential decrease in permeate TDS was recorded when input pressure was increased. Gude (2011) concluded that pressure increase has a positive impact on several parameters like salt rejection, recovery ratio and energy consumption.

The results in Figure. 9 show that a slight increase in pH led to a decrease in permeate TDS. The product quality improved dramatically with a slight increase in pH. Vaseghi et al. (2016) are in agreement with this phenomenon as they

state that pH varies inversely proportional to permeate TDS, where lower ion concentration is achieved when pH increases. However, an increase in feed pH resulted in an increase in permeate TDS for low flow rates, as is recorded by Alahmad (2010). Su et al. reiterate that pH variations generally have no effect on permeate TDS, because with an increase in pH cation rejection decreases while anion rejection increases (Su et al., 2017). Park and Kwon (2018) state that variations in pH have not yet been well understood; salt passage and permeate flux is higher in low and high pH due to membrane swelling.

6. CONCLUSIONS

WAVE simulation and optimization resulted in the theoretical improvement of the plant. Increasing the feed flow rate to about 24 m^3/h on the train resulted in 86 % production capacity, an increase of about 18 % towards achieving the design capacity of the plant. This was necessitated without changing the membranes or recovery ratio of the plant. SEC optimization, which is the chief objective of optimization, also resulted in a 7.3 % improvement in energy consumption, a reduction of about 0.48 kWh/m^3. Feed pressure of the system was also reduced to 50.5 bar from an average of about 55 bar in operation in the plant previously. Reduction in feed pressure led to a reduction in SEC, also leading to a reduction in total running costs of the plant (Appendix B), as compared to the simulated total running costs (Appendix A).

ACKNOWLEDGEMENTS

The author would like to acknowledge Nico-Ben Janse van Rensburg and the Quality Filtration System team for allowing him to use their facility and extract data for the research project.

REFERENCES

1. *Ahmed, F. E., Hashaikeh, R., Diabat, A., & Hilal, N. (2019). Mathematical and optimization modelling in desalination: State-of-the-art and future direction. Desalination, 469, 114092. DOI: https://doi.org/10.1016/j.desal.2019.114092*
2. *Randy Ncube & Freddie L. Inambao, "Experimental Data Analysis for a Reverse Osmosis Desalination Plant",International Journal of Mechanical and Production Engineering Research and Development (IJMPERD),Vol. 11, Issue 3,pp, 421-440*
3. *Alahmad, M. (2010). Prediction of performance of sea water reverse osmosis units. Desalination, 261(1-2), 131-137. DOI: https://doi.org/10.1016/j.desal.2010.05.018*
4. *Randy Ncube & Professor Freddie L. Inambao, "Theoretical Data Analysis for a Small-Scale Reverse Osmosis Desalination Plant",International Journal of Mechanical and Production Engineering Research and Development (IJMPERD),Vol. 11, Issue 2,pp, 31-40*
5. *Altaee, A.. (2012). Computational model for estimating reverse osmosis system design and performance: Part-one binary feed solution. Desalination, 291, 101-105. DOI: https://doi.org/10.1016/j.desal.2012.01.028*
6. *S. R. Kalbande, Priyanka Nayak, Sneha Deshmukh & V. P. Khambalkar, "Thermal Evaluation of Solar Water Desalination System with Evacuated Tubes",International Journal of Applied and Natural Sciences (IJANS),Vol. 6, Issue 1,pp; 41-54*
7. *Ang, W. & Mohammad, A. (2015. Mathematical modeling of membrane operations for water treatment. In A. Basile, A. Cassano, & N. K. Rastogi (Eds.), Advances in membrane technologies for water treatment (pp. 379-407), Woodhead Publishing.*
8. *K. K. Matrawy, "Modeling and Performance Evaluation of an Indirect Solar Desalination System",International Journal of Mechanical Engineering (IJME),Vol. 6, Issue 4,pp; 1-14*

9. *Assad, M. E. H., Al-Shabi, M., & Khaled. F. (2020). Reverse osmosis with an energy recovery device for seawater desalination powered by Geothermal energy. In 2020 Advances in Science and Engineering Technology International Conferences (ASET). pp. 1-5. IEEE.*

10. *Atab, M. S., Smallbone, A., & Roskilly, A. (2016). An operational and economic study of a reverse osmosis desalination system for potable water and land irrigation. Desalination, 397, 174-184. DOI: https://doi.org/10.1016/j.desal.2016.06.020*

11. *Atab, M. S., Smallbone, A., & Roskilly, A. (2018). A hybrid reverse osmosis/adsorption desalination plant for irrigation and drinking water. Desalination, 444, 44-52. DOI: https://doi.org/10.1016/j.desal.2018.07.008*

12. *Djebedjian, B., Gad, H., Khaled, I., & Rayan. M. A. (2008). Optimization of reverse osmosis desalination system using genetic algorithms technique. In Twelfth International Water Technology Conference, IWTC12, Alexandria, Egypt.*

13. *Du, J. R., Zhang, X., Feng, X., Wu, Y., Cheng, F., & Ali, M. E. (2020). Desalination of high salinity brackish water by an NF-RO hybrid system. Desalination, 491, 114445. DOI: https://doi.org/10.1016/j.desal.2020.114445*

14. *DuPont. (2021). WAVE Design Software. Available from: https://www.dupont.com/water/resources/design-software.html*

15. *Edina, M. (2017). New design software integrates three technologies into one tool. Available from: https://corporate.dow.com/en-us/news/press-releases/new-design-software-integrates-three-technologies-into-one-tool.html*

16. *Enqvist, J. P. & Ziervogel, G. (2019). Water governance and justice in Cape Town: An overview. Wiley Interdisciplinary Reviews: Water, 6(4), e1354. DOI: https://doi.org/10.1002/wat2.1354*

17. *Gandhidasan, P. & Al-Mojel, S. A. (2009). Effect of feed pressure on the performance of the photovoltaic powered reverse osmosis seawater desalination system. Renewable Energy, 34(12), 2824-2830. DOI: https://doi.org/10.1016/j.renene.2009.04.029*

18. *Gilabert Oriol, G., Hassan, M., Dewisme, J., Busch, M., & Garcia-Molina, V. (2013). High efficiency operation of pressurized ultrafiltration for seawater desalination based on advanced cleaning research. Industrial & Engineering Chemistry Research, 52(45), 15939-15945. DOI: https://doi.org/10.1021/ie402643z*

19. *Gude, V. G. (2011). Energy consumption and recovery in reverse osmosis. Desalination and Water Treatment, 36(1-3), 239-260. DOI: https://doi.org/10.5004/dwt.2011.2534*

20. *Guler, E., Ozakdag, D., Arda, M., Yuksel, M., & Kabay, N. (2010). Effect of temperature on seawater desalination-water quality analyses for desalinated seawater for its use as drinking and irrigation water. Environmental Geochemistry and Health, 32(4), 335-339. DOI: 10.1007/s10653-010-9294-x.*

21. *Jiang, A., Q. Ding, Q., Wang, J., Jiangzhou, S., Cheng, W., & Xing, C. (2014). Mathematical modeling and simulation of SWRO process based on simultaneous method. Journal of Applied Mathematics, 2014. DOI: http://dx.doi.org/10.1155/2014/908569*

22. *Khalifa, A., Ahmad, H., Antar, M., Laoui, T., & Khayet, M. (2017). Experimental and theoretical investigations on water desalination using direct contact membrane distillation. Desalination, 404, 22-34. DOI: https://doi.org/10.1016/j.desal.2016.10.009*

23. *Kim, S. J., Lee, Y. G., Oh, S., Lee, Y. S., Kim, Y. M., Jeon, M. G., Lee, S., Kim, I. S. & Kim, J. H. Energy saving methodology for the SWRO desalination process: Control of operating temperature and pressure. Desalination, 247(1-3), 260-270. DOI: https://doi.org/10.1016/j.desal.2008.12.006*

24. *Kim, J., Park, K., & Hong, S. (2020). Application of two-stage reverse osmosis system for desalination of high-salinity and high-temperature seawater with improved stability and performance. Desalination, 492, 114645. DOI:*

https://doi.org/10.1016/j.desal.2020.114645

25. *Kim, J., Park, K., Yang, D. R., & Hong, S. A comprehensive review of energy consumption of seawater reverse osmosis desalination plants. Applied Energy, 254, 113652. DOI: https://doi.org/10.1016/j.apenergy.2019.113652*
26. *Kim, S. J., Oh, S., Lee, Y. G., Jeon, M. G., Kim, I. S., & Kim, J. H. (2009). A control methodology for the feed water temperature to optimize SWRO desalination process using genetic programming. Desalination, 247(1-3), 190-199. DOI: https://doi.org/10.1016/j.desal.2008.12.024*
27. *Koutsou, C., Kritikos, E., Karabelas, A., & Kostoglou, M. (2020). Analysis of temperature effects on the specific energy consumption in reverse osmosis desalination processes. Desalination, 476, 114213. DOI: https://doi.org/10.1016/j.desal.2019.114213*
28. *Lappalainen, J., Korvola, T., & Alopaeus, V. (2017). Modelling and dynamic simulation of a large MSF plant using local phase equilibrium and simultaneous mass, momentum, and energy solver. Computers & Chemical Engineering, 97, 242-258. DOI: https://doi.org/10.1016/j.compchemeng.2016.11.039*
29. *Lee, C.-J., Chen, Y.-S., & Wang, G.-B. (2010). A dynamic simulation model of reverse osmosis desalination systems. In The 5th International Symposium on Design, Operation and Control of Chemical Processes, PSE ASIA, Singapore. 2010.*
30. *Lee, J. J., Woo, Y. C., & Kim, H.-S. (2015). Effect of driving pressure and recovery rate on the performance of nanofiltration and reverse osmosis membranes for the treatment of the effluent from MBR. Desalination and Water Treatment, 54(13), 3589-3595. DOI: https://doi.org/10.1080/19443994.2014.923196*
31. *Libotean, D., Giralt, J., Giralt, F., Rallo, R., Wolfe, T., & Cohen, Y. (2009). Neural network approach for modeling the performance of reverse osmosis membrane desalting. Journal of Membrane Science, 326(2), 408-419. DOI: https://doi.org/10.1016/j.memsci.2008.10.028*
32. *Murthy, Z. & Vengal, J. C. (2006). Optimization of a reverse osmosis system using genetic algorithm. Separation Science and Technology, 41(4), 647-663. DOI: 10.1080/01496390500526854*
33. *Nisan, S., Commercon, B., & Dardour, S. (20050. A new method for the treatment of the reverse osmosis process, with preheating of the feedwater. Desalination, 182(1-3), 483-495. DOI: https://doi.org/10.1016/j.desal.2005.02.041*
34. *Oh, H.-J., Hwang, T.-M., & Lee, S. (2009). A simplified simulation model of RO systems for seawater desalination. Desalination, 238(1-3), 128-139. DOI: https://doi.org/10.1016/j.desal.2008.01.043*
35. *Park, H.-G. & Kwon, Y.-N. (2018). Investigation on the factors determining permeate pH in reverse osmosis membrane processes. Desalination, 430, 147-158. DOI: https://doi.org/10.1016/j.desal.2017.12.060*
36. *Poullikkas, A. (2001). Optimization algorithm for reverse osmosis desalination economics. Desalination, 133(1), 75-81 DOI: https://doi.org/10.1016/S0011-9164(01)00084-4.*
37. *Sassi, K. M. & Mujtaba, I. M. (2010). Simulation and optimization of full scale reverse osmosis desalination plant.Computer Aided Chemical Engineering, 28, 895-900. DOI: https://doi.org/10.1016/S1570-7946(10)28150-6*
38. *Sassi, K. M. & Mujtaba, I. M. (2011). Optimal design and operation of reverse osmosis desalination process with membrane fouling. Chemical Engineering Journal, 171(2), 582-593. DOI: https://doi.org/10.1016/j.cej.2011.04.034*
39. *Su, X., Song, Y., Li, T., & Gao, C. (2017). Effect of feed water characteristics on nanofiltration separating performance for brackish water treatment in the Huanghuai region of China. Journal of Water Process Engineering, 19, 147-155. DOI: https://doi.org/10.1016/j.jwpe.2017.07.021*

40. *Swartz, C., Du Plessis, J., Burger, A., & Offringa, G. (2006). A desalination guide for South African municipal engineers. Water SA, 32(5). DOI: 10.4314/wsa.v32i5.47845*

41. *Vaseghi, G., Ghassemi, A., & Loya, J. (2016). Characterization of reverse osmosis and nanofiltration membranes: Effects of operating conditions and specific ion rejection. Desalination and Water Treatment, 57(50), 23461-23472. DOI: https://doi.org/10.1080/19443994.2015.1135825*

42. *Zarai, N., Tadeo, F., & Chaabene, M. (2013). Planning of the operating points in desalination plants based on energy optimization. International Journal of Computer Applications, 68(18), Available from: http://citeseerx.ist.psu.edu/viewdoc/download?doi=10.1.1.403.6874&rep=rep1&type=pdf*

APPENDIX

A: 110-10 Train Detailed Simulation Report

DUPONT

WATER APPLICATION VALUE ENGINE
WATER SOLUTIONS

RO Detailed Report

RO System Flow Diagram

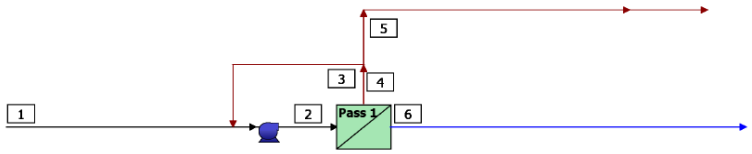

#	Description	Flow (m^3/h)	TDS (mg/L)	Pressure (bar)
1	Raw Feed to RO System	64.5	33,619	0.0
2	Net Feed to Pass 1	69.3	34,748	47.0
3	Concentrate Recycle from Pass 1 to Pass 1	4.94	48,753	44.1
4	Total Concentrate from Pass 1	49.4	48,752	44.1
5	Net Concentrate from RO System	44.4	48,752	44.1
6	Net Product from RO System	20.0	104.8	0.0

RO System Overview

Total # of Trains	1	Online =	1	Standby =	0	RO Recovery	31.0 %
System Flow Rate	(m^3/h)	Net Feed =	64.5	Net Product =	20.0		

Pass		Pass 1
Stream Name		Stream 1
Water Type		Sea Water (With conventional pretreatment, SDI < 5)
Number of Elements		42
Total Active Area	(m^2)	1717
Feed Flow per Pass	(m^3/h)	69.3
Feed TDS[a]	(mg/L)	34,748
Feed Pressure	(bar)	47.0
Flow Factor Per Stage		0.85
Permeate Flow per Pass	(m^3/h)	20.0
Pass Average flux	(LMH)	11.6
Permeate TDS[a]	(mg/L)	104.8
Pass Recovery		28.9 %
Average NDP	(bar)	14.1
Specific Energy	(kWh/m^3)	5.68
Temperature	(°C)	14.0
pH		7.2
Chemical Dose		-
RO System Recovery		31.0 %
Net RO System Recovery		31.0%

Footnotes:

[a]Total Dissolved Solids includes ions, SiO_2 and $B(OH)_3$. It does not include NH_3 and CO_2

RO Flow Table (Stage Level) - Pass 1

Stage	Elements	#PV	#Els per PV	Feed				Concentrate			Permeate			
				Feed Flow (m³/h)	Recirc Flow (m³/h)	Feed Press (bar)	Boost Press (bar)	Conc Flow (m³/h)	Conc Press (bar)	Press Drop (bar)	Perm Flow (m³/h)	Avg Flux (LMH)	Perm Press (bar)	Perm TDS (mg/L)
1	SW30XLE-440i	6	7	69.3	4.94	46.7	0.0	49.4	44.1	2.5	20.0	11.6	3.0	104.8

RO Solute Concentrations - Pass 1

Concentrations (mg/L as ion)						
		Adjusted Feed		Concentrate	Permeate	
	Raw Feed	Initial	After Recycle	Stage1	Stage1	Total
NH_4^+	0.00	0.00	0.00	0.00	0.00	0.00
K^+	0.00	0.00	0.00	0.00	0.00	0.00
Na^+	9,928	9,928	10,260	14,394	38.22	38.22
Mg^{+2}	1,654	1,654	1,709	2,400	1.60	1.60
Ca^{+2}	441.0	441.0	455.8	639.9	0.42	0.42
Sr^{+2}	0.00	0.00	0.00	0.00	0.00	0.00
Ba^{+2}	0.00	0.00	0.00	0.00	0.00	0.00
CO_3^{-2}	0.00	0.00	0.00	0.00	0.00	0.00
HCO_3^-	0.00	0.00	0.00	0.00	0.00	0.00
NO_3^-	0.00	0.00	0.00	0.00	0.00	0.00
F^-	0.00	0.00	0.00	0.00	0.00	0.00
Cl^-	18,997	18,997	19,632	27,546	63.70	63.69
Br^{-1}	0.00	0.00	0.00	0.00	0.00	0.00
SO_4^{-2}	2,600	2,600	2,687	3,773	0.90	0.90
PO_4^{-3}	0.00	0.00	0.00	0.00	0.00	0.00
SiO_2	0.00	0.00	0.00	0.00	0.00	0.00
Boron	0.00	0.00	0.00	0.00	0.00	0.00
CO_2	0.00	0.00	0.00	0.00	0.00	0.00
TDS[#]	33,619	33,619	34,744	48,752	104.8	104.8
Est. Cond. µS/cm	50,408	50,408	51,883	69,718	223	223
pH	7.2	7.2	7.2	7.3	7.2	7.2

Footnotes:

[#]Total Dissolved Solids includes ions, SiO_2 and $B(OH)_3$. It does not include NH_3 and CO_2

RO Design Warnings

None

Special Comments

Product	Special Comments
SW30XLE-440i	Consult your DuPont representative for advice on applications above 95°F (35°C).

RO Flow Table (Element Level) - Pass 1

DUPONT

WATER APPLICATION VALUE ENGINE
WATER SOLUTIONS

Stage	Element	Element Name	Recovery (%)	Feed Flow (m^3/h)	Feed Press (bar)	Feed TDS (mg/L)	Conc Flow (m^3/h)	Perm Flow (m^3/h)	Perm Flux (LMH)	Perm TDS (mg/L)
1	1	SW30XLE-440i	5.9	11.6	46.7	34,744	10.9	0.69	16.8	63.68
1	2	SW30XLE-440i	5.6	10.9	46.2	36,930	10.3	0.61	14.9	75.40
1	3	SW30XLE-440i	5.2	10.3	45.8	39,116	9.73	0.54	13.1	89.82
1	4	SW30XLE-440i	4.8	9.73	45.4	41,263	9.26	0.47	11.4	107.6
1	5	SW30XLE-440i	4.3	9.26	45.1	43,333	8.86	0.40	9.8	129.7
1	6	SW30XLE-440i	3.9	8.86	44.7	45,290	8.52	0.34	8.4	157.1
1	7	SW30XLE-440i	3.4	8.52	44.4	47,104	8.23	0.29	7.1	191.3

Footnotes:

[a]Total Dissolved Solids includes ions, SiO_2 and $B(OH)_3$. It does not include NH_3 and CO_2

RO Solubility Warnings

None

RO Chemical Adjustments

	Pass 1 Feed	RO 1st Pass Conc
pH	7.2	7.3
Langelier Saturation Index	0.00	0.00
Stiff & Davis Stability Index	0.00	0.00
TDS[a] (mg/l)	33,619	48,752
Ionic Strength (molal)	0.72	1.06
HCO_3^- (mg/L)	0.00	0.00
CO_2 (mg/l)	0.00	0.00
CO_3^{-2} (mg/L)	0.00	0.00
$CaSO_4$ (% saturation)	22.4	35.1
$BaSO_4$ (% saturation)	0.00	0.00
$SrSO_4$ (% saturation)	0.00	0.00
CaF_2 (% saturation)	0.00	0.00
SiO_2 (% saturation)	0.00	0.00
$Mg(OH)_2$ (% saturation)	0.01	0.02

Footnotes:

[a]Total Dissolved Solids includes ions, SiO_2 and $B(OH)_3$. It does not include NH_3 and CO_2

RO Utility and Chemical Costs

Service Water

	Flow Rate (m^3/h)	Unit Cost ($/m^3)	Hourly Cost ($/h)	Daily Cost ($/d)
Non-Product Feed Water				
Pass 1	44.4	0.1400	6.22	149.29
Total Non-product Feed Water Cost	44.4		6.22	149.29
Waste Water Disposal				
Pass 1	44.4	0.6900	30.66	735.76
Total Waste Water Disposal	44.4		30.66	735.76
Total Service Water Cost				885.05

WAVE Version: 1.81.814

Project Name: 100-10 Train Case: Case 1 Created: 04/05/2021 Page 4 of 5

Electricity

Peak Power	(kW)	113.5
Energy	(kWh/d)	2,724
Electricity Unit Cost	($/kWh)	0.0900
Electricity Cost	($/d)	245.2
Specific Energy	(kWh/m³)	5.68

Pump	Flow Rate (m³/h)	Power (kW)	Energy (kWh/d)	Cost ($/d)
Pass 1				
Feed	69.33	113.52	2,724.39	245.20
Pass 1 Total		113.52	2,724.39	245.20
System Total		113.52	2,724.39	245.20

Chemical

Chemical	Unit Cost ($/kg)	Dose (mg/L)	Volume (L/d)	Cost ($/d)
Total Chemical Cost				0.0

Utility and Chemical Cost	($/d)	1,130
Specific Water Cost	($/m³)	2.355

Appendix B: Detailed Optimization Report of the 100-10 Train

DUPONT

WATER APPLICATION VALUE ENGINE
WATER SOLUTIONS

RO Detailed Report

RO System Flow Diagram

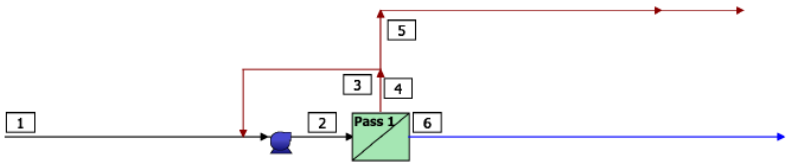

#	Description	Flow (m³/h)	TDS (mg/L)	Pressure (bar)
1	Raw Feed to RO System	77.4	33,619	0.0
2	Net Feed to Pass 1	83.2	34,752	50.5
3	Concentrate Recycle from Pass 1 to Pass 1	5.92	48,766	46.9
4	Total Concentrate from Pass 1	59.2	48,767	46.9
5	Net Concentrate from RO System	53.3	48,767	46.9
6	Net Product from RO System	24.0	82.80	0.0

RO System Overview

Total # of Trains	1	Online =	1	Standby =	0	RO Recovery	31.0 %
System Flow Rate	(m³/h)	Net Feed =	77.4	Net Product =	24.0		

Pass		Pass 1
Stream Name		Stream 1
Water Type		Sea Water (With conventional pretreatment, SDI < 5)
Number of Elements		42
Total Active Area	(m²)	1717
Feed Flow per Pass	(m³/h)	83.2
Feed TDS[a]	(mg/L)	34,752
Feed Pressure	(bar)	50.5
Flow Factor Per Stage		0.85
Permeate Flow per Pass	(m³/h)	24.0
Pass Average flux	(LMH)	14.0
Permeate TDS[a]	(mg/L)	82.80
Pass Recovery		28.8 %
Average NDP	(bar)	17.3
Specific Energy	(kWh/m³)	6.10
Temperature	(°C)	13.0
pH		7.3
Chemical Dose		-
RO System Recovery		31.0 %
Net RO System Recovery		31.0%

Footnotes:

[a]Total Dissolved Solids includes ions, SiO_2 and $B(OH)_3$. It does not include NH_3 and CO_2

WAVE Version: 1.81.814

Project Name: 100-10 Train Optimization Case: Case 1 Created: 04/05/2021 Page 2 of 5

RO Flow Table (Stage Level) - Pass 1

Stage	Elements	#PV	#Els per PV	Feed				Concentrate			Permeate			
				Feed Flow (m³/h)	Recirc Flow (m³/h)	Feed Press (bar)	Boost Press (bar)	Conc Flow (m³/h)	Conc Press (bar)	Press Drop (bar)	Perm Flow (m³/h)	Avg Flux (LMH)	Perm Press (bar)	Perm TDS (mg/L)
1	SW30XLE-440i	6	7	83.2	5.92	50.2	0.0	59.2	46.9	3.4	24.0	14.0	3.0	82.80

RO Solute Concentrations - Pass 1

Concentrations (mg/L as ion)						
	Raw Feed	Adjusted Feed		Concentrate	Permeate	
		Initial	After Recycle	Stage1	Stage1	Total
NH_4^+	0.00	0.00	0.00	0.00	0.00	0.00
K^+	0.00	0.00	0.00	0.00	0.00	0.00
Na^+	9,928	9,928	10,261	14,399	30.18	30.18
Mg^{+2}	1,654	1,654	1,710	2,401	1.27	1.27
Ca^{+2}	441.0	441.0	455.8	640.0	0.33	0.33
Sr^{+2}	0.00	0.00	0.00	0.00	0.00	0.00
Ba^{+2}	0.00	0.00	0.00	0.00	0.00	0.00
CO_3^{-2}	0.00	0.00	0.00	0.00	0.00	0.00
HCO_3^-	0.00	0.00	0.00	0.00	0.00	0.00
NO_3^-	0.00	0.00	0.00	0.00	0.00	0.00
F^-	0.00	0.00	0.00	0.00	0.00	0.00
Cl^-	18,997	18,997	19,635	27,555	50.31	50.31
Br^{-1}	0.00	0.00	0.00	0.00	0.00	0.00
SO_4^{-2}	2,600	2,600	2,687	3,773	0.71	0.71
PO_4^{-3}	0.00	0.00	0.00	0.00	0.00	0.00
SiO_2	0.00	0.00	0.00	0.00	0.00	0.00
Boron	0.00	0.00	0.00	0.00	0.00	0.00
CO_2	0.00	0.00	0.00	0.00	0.00	0.00
TDS[a]	33,619	33,619	34,749	48,767	82.80	82.80
Est. Cond. µS/cm	50,408	50,408	51,889	69,737	177	177
pH	7.3	7.3	7.3	7.3	7.2	7.2

Footnotes:

[a]Total Dissolved Solids includes ions, SiO_2 and $B(OH)_3$. It does not include NH_3 and CO_2

RO Design Warnings

None

Special Comments

Product	Special Comments
SW30XLE-440i	Consult your DuPont representative for advice on applications above 95°F (35°C).

RO Flow Table (Element Level) - Pass 1

DUPONT

WATER APPLICATION VALUE ENGINE
WATER SOLUTIONS

Stage	Element	Element Name	Recovery (%)	Feed Flow (m^3/h)	Feed Press (bar)	Feed TDS (mg/L)	Conc Flow (m^3/h)	Perm Flow (m^3/h)	Perm Flux (LMH)	Perm TDS (mg/L)
1	1	SW30XLE-440i	5.7	13.9	50.2	34,749	13.1	0.78	19.2	52.74
1	2	SW30XLE-440i	5.4	13.1	49.6	36,826	12.4	0.71	17.3	61.33
1	3	SW30XLE-440i	5.1	12.4	49.1	38,928	11.7	0.64	15.5	71.67
1	4	SW30XLE-440i	4.8	11.7	48.6	41,026	11.2	0.56	13.8	84.18
1	5	SW30XLE-440i	4.5	11.2	48.1	43,090	10.7	0.50	12.2	99.36
1	6	SW30XLE-440i	4.1	10.7	47.7	45,087	10.2	0.43	10.6	117.9
1	7	SW30XLE-440i	3.7	10.2	47.2	46,988	9.87	0.38	9.2	140.5

Footnotes:

[a]Total Dissolved Solids includes ions, SiO_2 and $B(OH)_3$. It does not include NH_3 and CO_2

RO Solubility Warnings

None

RO Chemical Adjustments

	Pass 1 Feed	RO 1st Pass Conc
pH	7.3	7.3
Langelier Saturation Index	0.00	0.00
Stiff & Davis Stability Index	0.00	0.00
TDS[a] (mg/l)	33,619	48,767
Ionic Strength (molal)	0.72	1.06
HCO_3^- (mg/L)	0.00	0.00
CO_2 (mg/l)	0.00	0.00
CO_3^{-2} (mg/L)	0.00	0.00
$CaSO_4$ (% saturation)	22.4	35.1
$BaSO_4$ (% saturation)	0.00	0.00
$SrSO_4$ (% saturation)	0.00	0.00
CaF_2 (% saturation)	0.00	0.00
SiO_2 (% saturation)	0.00	0.00
$Mg(OH)_2$ (% saturation)	0.01	0.02

Footnotes:

[a]Total Dissolved Solids includes ions, SiO_2 and $B(OH)_3$. It does not include NH_3 and CO_2

RO Utility and Chemical Costs

Service Water

	Flow Rate (m^3/h)	Unit Cost ($/m^3)	Hourly Cost ($/h)	Daily Cost ($/d)
Non-Product Feed Water				
Pass 1	53.3	0.1400	7.46	179.08
Total Non-product Feed Water Cost	53.3		7.46	179.08
Waste Water Disposal				
Pass 1	53.3	0.6900	36.77	882.60
Total Waste Water Disposal	53.3		36.77	882.60
Total Service Water Cost				1061.68

WAVE Version: 1.81.814

Project Name: 100-10 Train Optimization Case: Case 1 Created: 04/05/2021 Page 4 of 5

Electricity

Peak Power	(kW)	146.5
Energy	(kWh/d)	3,515
Electricity Unit Cost	($/kWh)	0.0900
Electricity Cost	($/d)	316.4
Specific Energy	(kWh/m³)	6.10

Pump	Flow Rate (m³/h)	Power (kW)	Energy (kWh/d)	Cost ($/d)
Pass 1				
Feed	83.17	146.46	3,515.09	316.36
Pass 1 Total		146.46	3,515.09	316.36
System Total		146.46	3,515.09	316.36

Chemical

Chemical	Unit Cost ($/kg)	Dose (mg/L)	Volume (L/d)	Cost ($/d)
Total Chemical Cost				0.0

Utility and Chemical Cost	($/d)	1,378
Specific Water Cost	($/m³)	2.393